The Effects of Binary Stars on Inferred Remnant Populations in Globular Clusters

by

Peter Smith

A THESIS SUBMITTED IN PARTIAL FULFILMENT OF
THE REQUIREMENTS FOR THE DEGREE OF

BACHELOR OF SCIENCE

in

Honours Astrophysics

(Department of Astronomy and Physics, Dr. Vincent Hénault-Brunet supervising faculty)

.....

.....

.....

.....

.....

SAINT MARY'S UNIVERSITY

February 25, 2022

Abstract

The Effects of Binary Stars on Inferred Remnant Populations in Globular Clusters

by *Peter Smith*

submitted on February 25, 2022:

Abstract Here

Contents

List of Figures

List of Tables

Chapter 1

Introduction

1.1 Globular Clusters

Globular clusters (GCs) are dense, spheroidal collections of hundreds of thousands of stars bound by their own self-gravity. GCs are found in most galaxies, with the Milky Way hosting roughly 150, mostly located in the outer halo (Heggie and Hut, 2003). GCs represent some of the oldest stellar populations in the universe and are usually in excess of 10 billion years old. Figure 1.1 shows the globular cluster NGC 7006, imaged by the Hubble Space Telescope's Advanced Camera for Surveys. The dense core of the cluster is clearly visible and is made up of tens of thousands of stars. The dynamics of globular clusters are almost entirely governed by the interactions between individual cluster members, with small effects from the galactic potential of its host galaxy as well as mass loss due to stellar evolution. Two-body relaxation is essentially the main driver of the evolution of GCs and through this process, they display a wide range of dynamical phenomena. Among these phenomena, mass segregation is a process through which heavier objects migrate to the centre of a cluster and lighter objects move to the outer regions. As objects interact with each other, their kinetic energies will tend to equalize which leads to heavier objects slowing down and lighter objects speeding up (Heggie and Hut, 2003). This process leads to the core of the cluster

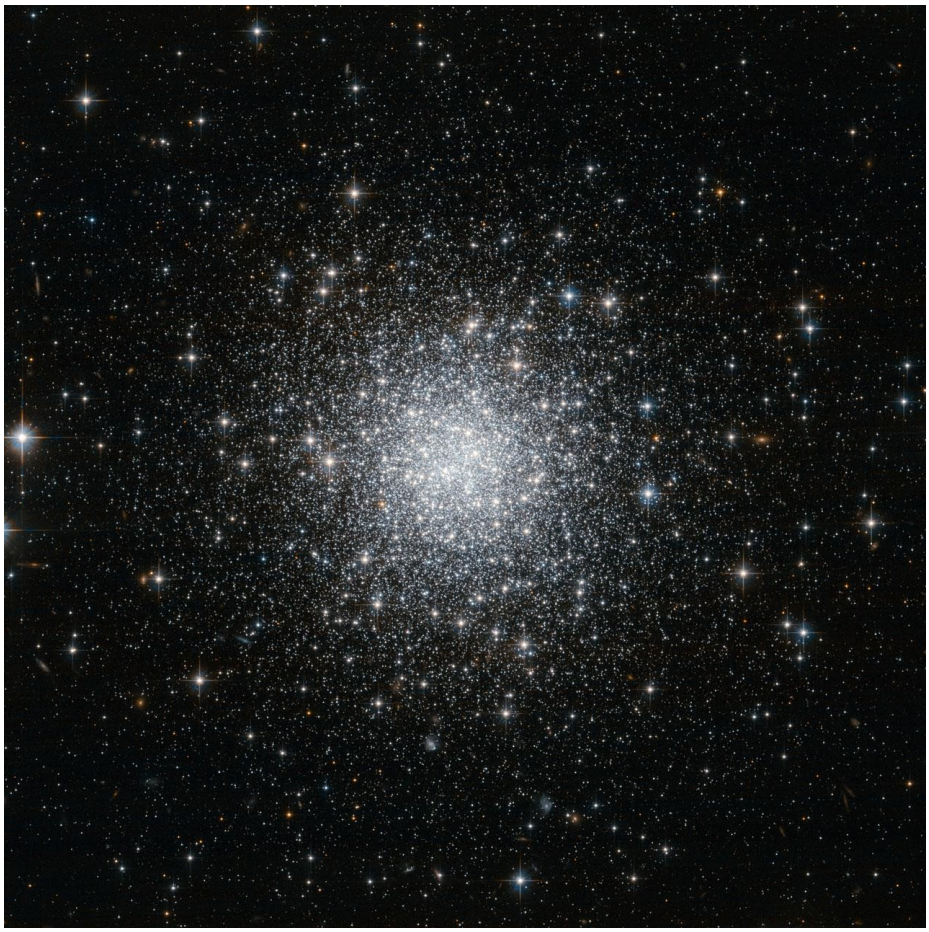

Figure 1.1: The globular cluster NGC 7006 imaged by the Hubble Space Telescope's Advanced Camera for Surveys, photo courtesy of ESA/Hubble & NASA

containing a much higher proportion of high-mass stars and heavy remnants than the rest of the cluster. Figure 1.2 shows the mean mass of objects within a realistic model of a globular cluster as a function of distance from the cluster centre. The regions closest to the core of the cluster have a much higher mean mass due to the increased presence of heavy remnants and high-mass stars caused by the effects of mass segregation.

The study of stellar remnants in globular clusters has far-reaching implications for diverse fields of astrophysics. Globular clusters are one of the most commonly

proposed candidates to host intermediate-mass black holes (IMBHs). Due to the effects of mass segregation and the high densities within the cores of globular clusters, the central regions of globular clusters are an ideal environment for mergers of compact objects (Rodriguez et al., 2021). These mergers can be detected through their resultant gravitational waves and the expected rates for gravitational wave events depend significantly on the compact object populations in globular clusters. These mergers are also thought to be one of the most promising formation channels for IMBHs (Giersz et al., 2015), a so-far undetected class of black holes whose masses fall between those of stellar-mass black holes and those of supermassive black holes. The formation of these black holes has important implications for understanding the formation of the supermassive black holes that we find at the centre of galaxies.

The work presented in this thesis builds on a previous project I worked on which used pulsar timing data to constrain the properties of the globular cluster 47 Tuc. In that work, we were able to place strong limits on the mass in dark remnants (black holes, neutron stars, white dwarfs) within the cluster, establishing strong constraints on the black hole content specifically. While this project was able to fully account for effects like mass segregation and uncertain mass functions, one limitation of the models that it used (which we will discuss in the following section) was the assumption that all objects within the cluster are single. Because the masses of some binary stars are higher than the typical masses of objects within the cluster, they too will mass segregate to the core of the cluster like heavy stellar remnants. While the binary fraction in 47 Tuc is expected to be quite low (Milone et al., 2012), the effects that a centrally concentrated population of binary stars might have on the inferred remnant

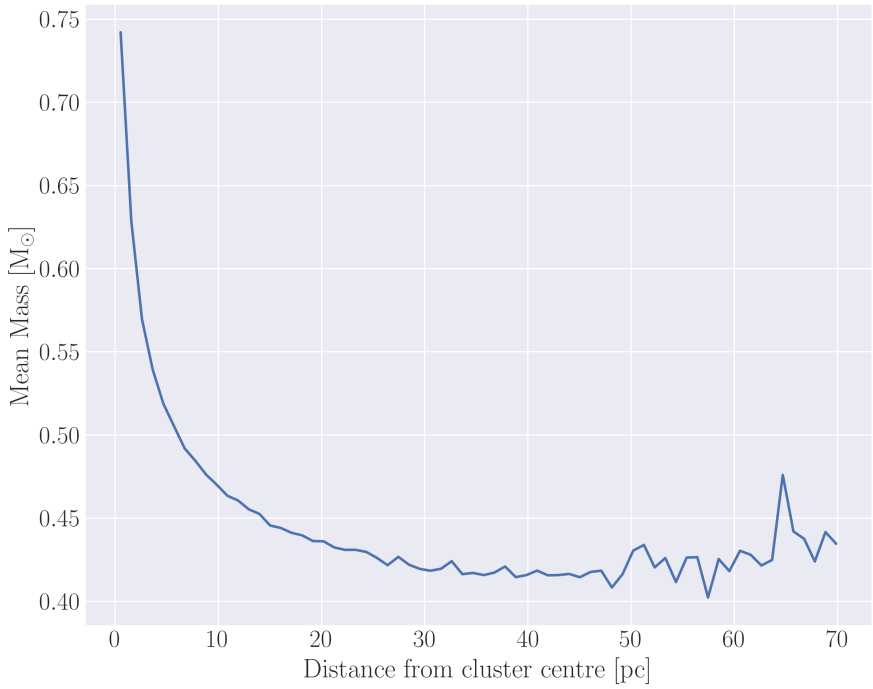

Figure 1.2: Mean mass of objects within a realistic model of the globular cluster 47 Tuc, as a function of distance from the cluster centre. The concentration of high-mass objects in the central regions of the cluster is obvious, as is the preference for low-mass objects in the outskirts of the cluster, clearly demonstrating the effects of mass segregation.

content of the cluster is still unclear and worth investigating.

1.2 Modelling Globular Clusters

When modelling the dynamics of globular clusters, there are generally two approaches commonly used. The first is to model the entire evolutionary history of the cluster from initial conditions to the present day. The most commonly employed versions of these "evolutionary models" are direct N-body integration (see for example Baumgardt 2017) which directly calculate the gravitational interactions between each object in the cluster and Monte Carlo models (e.g. Rodriguez et al. 2021, Hypki

and Giersz 2013) which approximate the gravitational interactions between objects according to the method of Hénon (1971). While these models provide insight into the dynamical history of the cluster, they are very computationally expensive with even the fastest models taking on the order of a day to model a realistic globular cluster (Rodriguez et al., 2021).

The second approach is to model just the present-day conditions of the cluster. These models, which we call "equilibrium models", capture none of the dynamical history of the cluster but fully describe the present-day state of the cluster. These equilibrium models are much less computationally demanding than evolutionary models. Their relative efficiency allows us to explore a significantly larger parameter space when fitting the models to observations to constrain the present-day properties of a cluster. In particular, it is worth highlighting that by using equilibrium models, we are able to vary the stellar mass function of the cluster as well as the black hole and remnant retention fractions with more flexibility than what might be possible with evolutionary models, due to the computational cost of computing extensive grids of evolutionary models with many parameters varied in the initial conditions (e.g. various stellar initial mass functions, initial cluster radii, masses, etc.).

The comparative efficiency of these models further enables the use of statistical fitting techniques like MCMC or Nested Sampling which would be prohibitively expensive to use with evolutionary models. This means that instead of computing a grid of models and finding the "best-fitting" model we can instead recover posterior distributions for key cluster parameters.

In this work, we use the `LIMEPY` family of models presented by Gieles and Zocchi

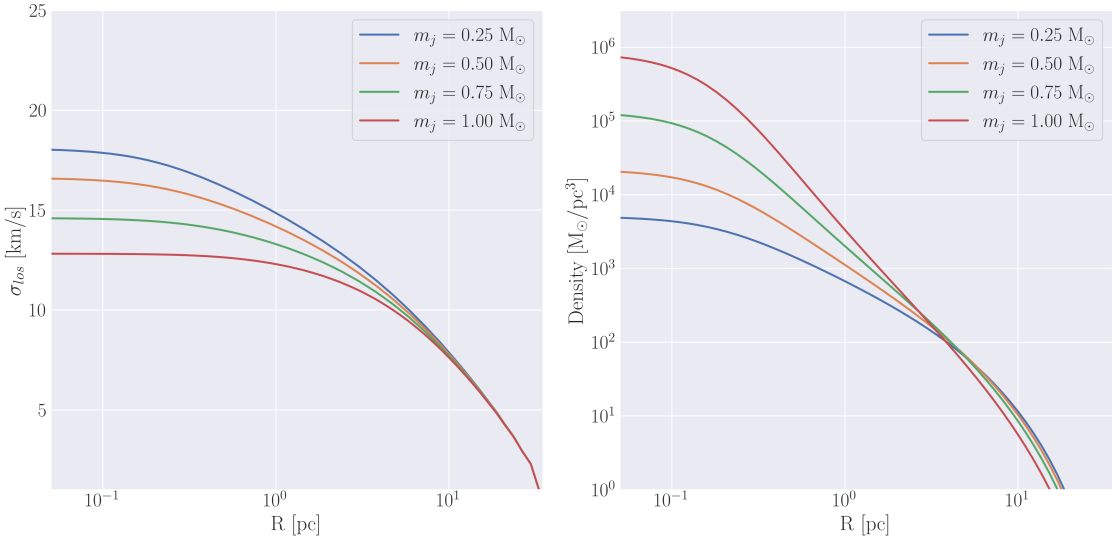

Figure 1.3: A simple `LIMEPY` model with four components with differing *mean* masses but equal *total* masses. The lighter components have higher velocity dispersions and are less centrally concentrated while the more massive components have lower velocity dispersions and are more centrally concentrated.

(2015). The `LIMEPY` models are a set of distribution function-based equilibrium models that are isothermal for the most bound stars near the cluster centre and described by polytropes in the outer regions near the escape energy. The models have been extensively tested against N-body models (Zocchi et al., 2016; Peuten et al., 2017) and are able to effectively reproduce the effects of mass segregation. Their suitability for mass modelling globular clusters has been tested on mock data (Hénault-Brunet et al., 2019) and they have recently been applied to real datasets as well (e.g. Gieles et al., 2018; Hénault-Brunet et al., 2020).

Figure 1.3 shows the density and velocity dispersion profiles for a simple `LIMEPY` model with four components. The lightest components have the highest velocity dispersion and the most massive components are the most centrally concentrated.

The input parameters needed to compute our models include the central concen-

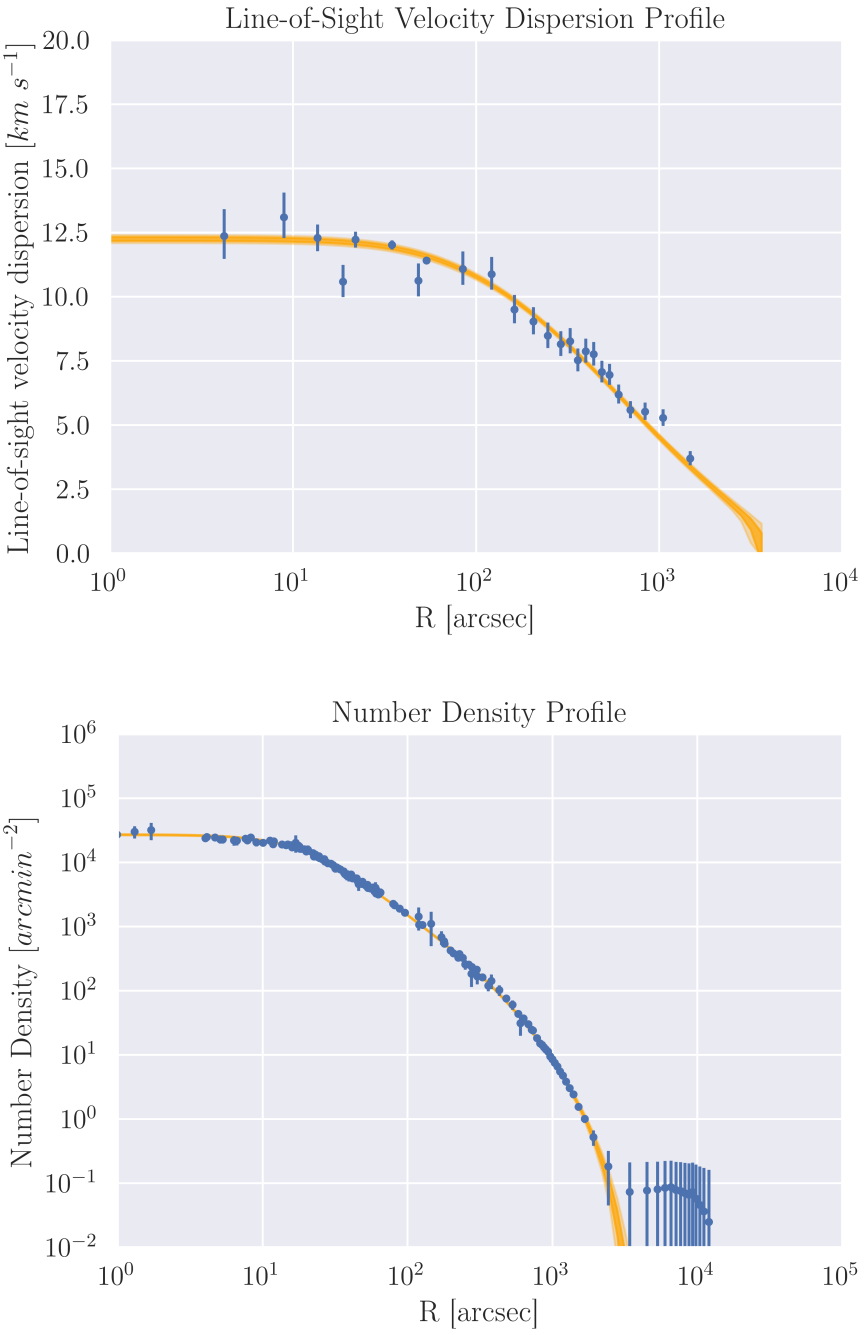

Figure 1.4: The line-of-sight velocity dispersion profile and number density profile of 47 Tuc, simultaneously fit by a `LIMEPY` model. The `LIMEPY` models are able to very accurately reproduce a range of cluster observables including simultaneous fitting of stellar mass function data and kinematic data.

tration parameter W_0, the truncation parameter g[1], the anisotropy radius r_a which determines the degree of radial anisotropy in the models, δ which sets the mass dependence of the velocity scale and thus governs the degree of mass segregation, and finally the specific mass bins to use as defined by the mean stellar mass (m_j) and total mass (M_j) of each bin, which together specify the stellar mass function. In order to scale the model units into physical units, the total mass of the cluster M and a size scale (the half-mass radius of the cluster r_h) are provided as well. Figure 1.4 demonstrates the ability of the models to simultaneously fit many cluster observables, specifically pictured are the line-of-sight velocity dispersion profile and the number density profile, though the power of these models lies in their ability to simultaneously fit not just kinematic and number density data but also the stellar mass function data of a cluster.

In their current implementation, these models assume that all objects within the cluster are single and make no attempt to model the dynamical effects of stellar multiplicity. In this project, we adapt these models to incorporate some of the effects of binary stars under the assumption that binaries with very long periods have been ionized by the present day. This allows us to treat binary systems as point masses and lets us model their dynamics by simply moving some of the mass in stars into heavier bins according to the specified binary population.

[1]Several well-known classes of models are reproduced by specific values of g: Woolley models (Woolley, 1954) have $g = 0$, King models (King, 1966) $g = 1$, and Wilson models (Wilson, 1975) $g = 2$.

1.3 Binary Stars

1.3.1 Binaries in Globular Clusters

In general, the binary systems found within present-day clusters differ significantly from the field binaries that are more easily observed. In particular, we expect very few long-period binaries, on account of them being ionized by the frequent interactions with other cluster members (Heggie and Hut, 2003). We frequently use the terms "hard" and "soft" to describe binaries where "soft binaries" have binding energies less than or comparable to the average kinetic energy of a cluster member while "hard binaries" have larger binding energies. Due to the frequent interactions within clusters, we expect that all soft binaries have long since been ionized by the present day leaving only a population of hard binaries with a truncated period distribution compared to field binaries (Heggie and Hut, 2003).

The most obvious way that binaries can affect the dynamics of a cluster is through three- or four-body interactions with other cluster members. When a single star (or another binary) interacts with a binary system at a close enough range, if the binary is hard, it will impart some of its energy to the ejected star and "harden" further. If the binary is soft, it will further "soften", potentially becoming unbound. Through these processes, soft binaries are slowly disrupted while hard binaries become harder (Heggie, 1975). Hard binary systems can act as a reserve of kinetic energy for a cluster through these three-body interactions with passing cluster members (Heggie and Hut, 2003). Binary stars are thought to be one of the primary mechanisms through which core-collapse (the collapse of the core of a cluster into extremely high density caused

by runaway mass segregation) is halted in some clusters by continually adding to the energy of stars which migrate to the central regions, thereby pushing them back out into the extended regions of the cluster (Chatterjee et al., 2013). Because the models that we will be focusing on do not model the evolutionary history of individual objects within the cluster, we will instead focus on the second way that binaries can affect the dynamics of a cluster.

Because binaries are tightly bound, for all interactions except for the very closest, they effectively act as a single point mass equal to the sum of each component's mass. In this way, binaries can affect cluster dynamics in much the same way that a large population of heavy remnants might. Much like black holes and neutron stars, binary systems will migrate to the centre of a cluster due to the effect of mass segregation. It has been found (e.g. Kremer et al. 2019) that a central population of black holes can fulfill a similar role to binary systems in halting core collapse by injecting kinetic energy through two-body interactions within the core of the cluster. This same mechanism could apply with tightly-bound binary systems that have mass-segregated to the centre of the cluster. This predicted increase in binary fraction as you get closer to the centre of a cluster is also seen in observations and is illustrated in Figure 1.5 for NGC 3201.

The effect of having a large central population of binaries could be that our models are overestimating the number of black holes and other high-mass objects (neutron stars, massive white dwarfs) in the core of the cluster. Because the gravitational potential in the central regions of the cluster is fairly well constrained by kinematic measurements, if we are missing a significant contribution from binaries, the models

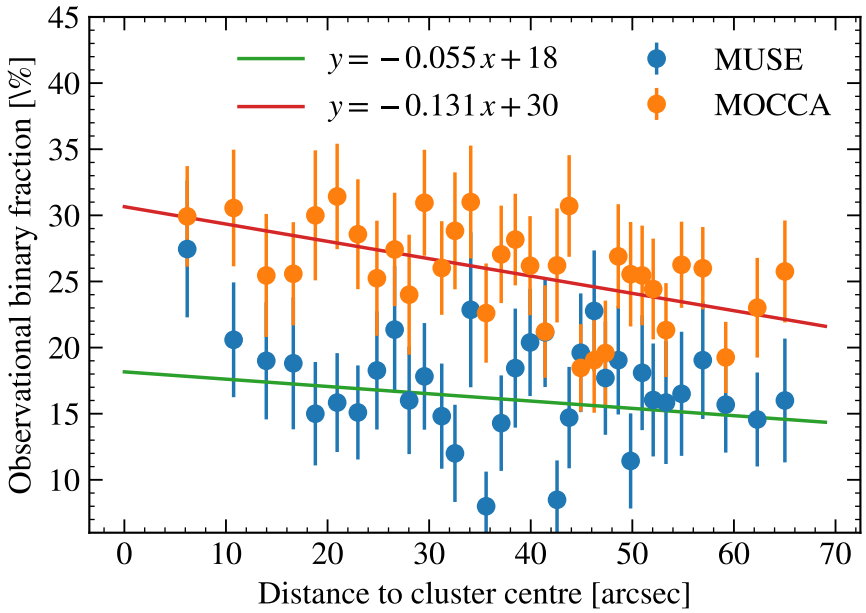

Figure 1.5: Observed binary fraction vs projected distance from cluster centre for NG 3201 as measure by the MUSE instrument. The slight trend in radial binary fraction is visible. Also plotted is the observed binary fraction in a MOCCA model which matches well with NGC 3201. MOCCA is a Monte Carlo model designed to model globular clusters for which there is a large grid of pre-computed models available. Reproduced from Figure 8 of Giesers et al. (2019).

may be compensating for this "missing mass" by adding more mass to the heavy end of the IMF which would lead to an overestimation of the number of neutron stars and black holes. By including realistic populations of binary stars in our models, we hope to recover more accurate remnant populations for present-day clusters.

1.3.2 Observations of Binary Stars in Globular Clusters

In general, there are two methods used to detect binaries within globular clusters: high-precision photometric observations and radial velocity surveys.

High-precision photometry can be used to detect binaries along the main sequence which have a significant difference in the mass of their components. We often use the ratio between the mass of the primary star and the companion star to quantify this difference: an equal mass binary will have a mass ratio of $q = 1$ while a binary with a large difference in the masses of its components will have a mass ratio closer to zero. Binaries that are detectable through this method typically have a mass ratio greater than $q = 0.5$. These systems will appear to be raised above the main sequence when plotted on a colour-magnitude diagram as their colour will match that of a typical main-sequence star however their luminosity will be the sum of each component. Figure 1.6 shows the main sequence of the cluster NGC 2298. The binary stars in this cluster are visible above the main sequence, raised according to their mass ratio. Milone et al. (2012) performed high-precision photometry on several globular clusters using the Hubble Space Telescope's (HST) Advanced Camera for Surveys and were able to place strong constraints on the binary fraction for binaries with a mass ratio above $q = 0.5$. This method allows for large studies of binary populations in GCs without the need for dedicated observations of individual systems but suffers from an inherent bias towards systems with high mass ratios. Systems with mass ratios below $q = 0.5$ are typically too close to the regular main-sequence to confidently classify as binaries (see Figure 1.6). This means that studies that employ this method must assume an underlying mass-ratio distribution for low values of q if they wish to place any limits on the overall binary fraction of a cluster. Typical values for the binary fraction in massive clusters found using this method range from almost zero to an upper limit of around 15% (Milone et al., 2012). Additionally, studies of the mass

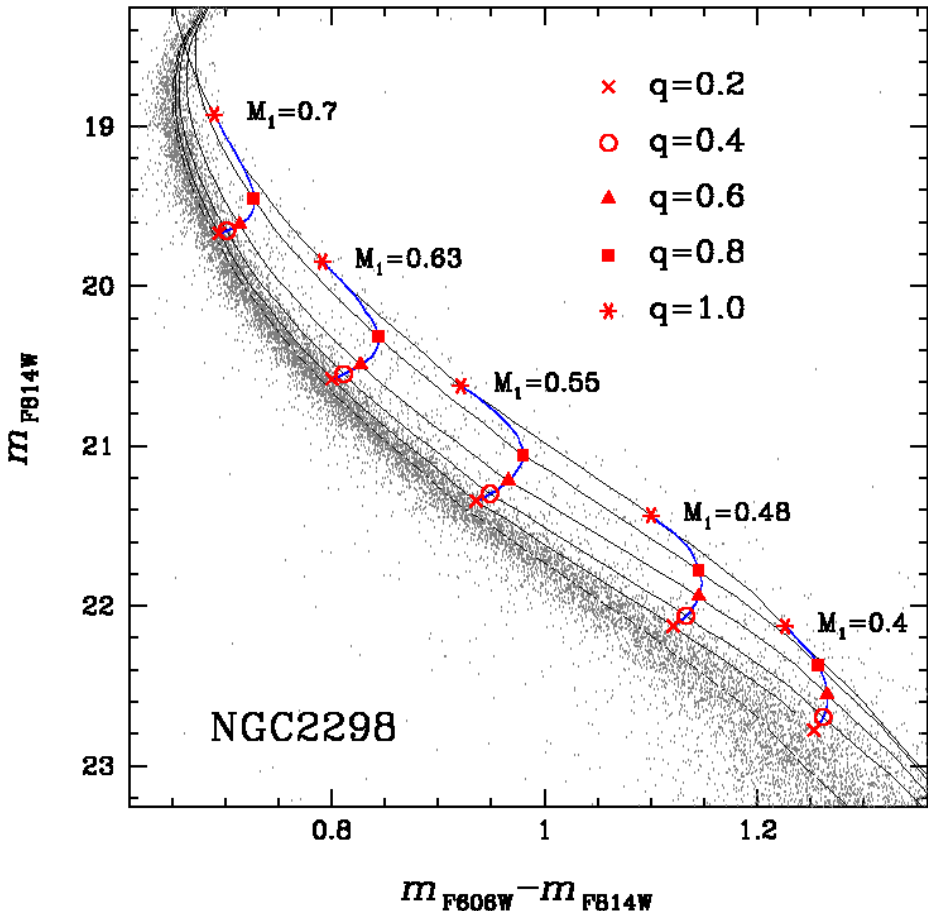

Figure 1.6: The main-sequence portion of the colour-magnitude diagram for NGC 2298. Binary systems are visible as being raised above the primary main sequence with systems with a higher mass ratio being raised further off of the main sequence. Systems below a mass ratio of $q = 0.5$ are nearly indistinguishable from the regular spread in main sequence stars. Reproduced from Figure 1 of Milone et al. (2012).

ratio distribution within these clusters using the same method find a preference for a uniform or "flat" distribution unlike the distribution in the solar neighbourhood which is peaked at $q = 1.0$ (Milone et al., 2012; Fisher et al., 2005)

Large-scale campaigns to measure the radial velocities for many stars in a cluster over many epochs are another method that can be used to detect binaries in GCs. Systems that are found to have periodically varying radial velocities can typically be

confidently classified as binary systems. Giesers et al. (2019) used the MUSE integral field spectrograph installed at the European Southern Observatory's Very Large Telescope to observe several GCs and reported the results for NGC 3201. Integral field spectrographs provide spatially resolved spectra for the entire field of view of the detector which enables far more time-efficient surveys than previous methods. Because this method measures radial velocities over time, periods for the binaries can be accurately determined and given enough measurements, many other parameters like eccentricity and companion mass can be accurately constrained in contrast to photometric methods which can only provide the mass ratio. This method also suffers from biases in that it requires the primary star of a binary to be bright enough to enable good spectroscopic measurements which may bias the sample towards systems with more massive primary stars. For NGC 3201, the binary fraction found using this method was $6.75 \pm 0.72\%$ (Giesers et al., 2019) which differs from the photometric estimates of Milone et al. (2012) which range from 10-12% for different fields.

The remainder of the thesis is structured as follows: in Chapter 2 I will describe the method used to generate mass functions which include realistic binary populations as well as the specifics of fitting these modified mass functions to real observations of stellar mass functions. Chapter 3 discusses the results of the simulations, including the differences between models with and without binaries. Chapter 4 discusses the overall implications of including binaries in our models, specifically when fitting them to observations.

Chapter 2

Methods

2.1 Data

We use a wide range of data to constrain the parameters of our models. In general, for both 47 Tuc and NGC 3201 we use archival kinematic data from ground based spectroscopy, number density profiles from *Gaia* and stellar mass function data from HST photometry.

2.1.1 Kinematics and density profiles

Proper motion dispersion profiles

For 47 Tuc, we use two sets of *Hubble Space Telescope* (HST) proper motion data that are not available for NGC 3201. To probe the inner regions of the cluster we use the proper motion dispersion profiles (both tangential and radial components) from Watkins et al. (2015) which are based on a catalogue of proper motions of bright stars from Bellini et al. (2014). These dispersion profiles are built from stars brighter than the main sequence turn-off (0.85 $M_\odot$ and 0.8 $M_\odot$ for 47 Tuc and NGC 3201). To probe the kinematics in the outer regions of the cluster, we also use the data from Heyl et al. (2017), for which the mean mass of the measured stars is 0.38 $M_\odot$. The outer proper motion data also allows us to constrain the amount of radial anisotropy

present in the cluster, which can mimic the effect of central dark mass in isotropic models by raising the central velocity dispersion (Zocchi et al., 2017).

Line-of-sight velocity dispersion profiles

For both 47 Tuc and NGC 3201 we use the line-of-sight velocity dispersion profiles from Baumgardt and Hilker (2018) to further constrain the kinematics of the clusters. These dispersion profiles are based on archival ESO/VLT and Keck spectra along with previously published radial velocity data from the literature. As these radial velocity samples are dominated by bright stars, we assume that the velocity dispersion profile traces the kinematics of upper main-sequence and evolved stars in our models.

Number density profiles

We use the number density profiles from De Boer et al. (2019) to constrain the size and structural parameters of the clusters. These profiles are made up of a combination of cluster members based on Gaia DR2 data in the outer regions and data from various literature sources in the central regions. The Gaia data used only includes bright stars ($m > 0.6$ M$_\odot$, for both clusters) and the literature data is dominated by bright stars, therefore in our models we assume the profiles probe the distribution of upper main sequence and evolved stars.

2.1.2 Stellar mass functions

As a constraint on the global present-day stellar mass function of the clusters, we use a compilation of HST based stellar mass function data from Baumgardt[1] (2021, priv. comm.), which represent an updated and augmented version of the stellar mass functions found in Sollima and Baumgardt (2017). This compilation is made up of several HST fields at varying distances from the cluster centre. These fields extend out to $14'$ and $8.33'$ from the cluster centres for 47 Tuc and NGC 3201 respectively and cover a mass range of $0.16 - 0.8$ $M_{\odot}$. The large radial and mass ranges allow us to constrain the degree mass segregation in the clusters.

2.1.3 Pulsar Data

For 47 Tuc, we make use of its large population of millisecond pulsars (MSPs) to place further constraints on its mass distribution. We use both the spin and orbital period timing solutions from Freire et al. (2017), Ridolfi et al. (2016) and Freire and Ridolfi (2018). We also consider the dispersion measures of the pulsars which, when combined with internal gas models from Abbate et al. (2018), allow us to constrain the line-of-sight position of the pulsars within the cluster. The work surrounding the use of pulsar data to constrain the models was performed as part of an earlier project and so will not be discussed in too much detail in this project.

[1] `https://people.smp.uq.edu.au/HolgerBaumgardt/globular/`

2.1.4 Binary Data

In order to create realistic binary populations we use the data from Milone et al. (2012) to inform our choices of binary fraction and mass ratio distribution. For 47 Tuc this means a flat mass ration distribution and a binary fraction of roughly 2% Peter: This is so small, do we want to use something larger for testing the effects?. For NGC 3201 Milone et al. (2012) find a binary fraction of around 10% with a flat mass ratio distribution while Giesers et al. (2019) find a value closer to $f_b = 0.0675$ without constraining the mass ratio distribution.

2.2 Generating mass functions

The bulk of project deals with generating mass functions to use as inputs to the `LIMEPY` models, we do this in two main steps, we first generate a present-day mass function comprised of only single stars, and we then modify it to include binary stars.

2.2.1 Single Star Mass Functions

Peter: More details here?

To generate the mass functions comprised of single stars we use the `evolve_mf` algorithm from `SSPTools`[2], a publicly available package for working with simple stellar populations.

The `evolve_mf` algorithm combines precomputed grids of stellar evolution models and isochrones to accurately model the evolution of a given initial mass function, fully

[2] `www.github.com/pjs902/ssptools`

including the effects of stellar evolution, mass loss due to escaping stars and dynamical ejections. The algorithm returns a sampled mass function for a requested time, ideal for use in the `LIMEPY` models.

We parameterize the mass function as a broken power-law with breakpoints at $0.5M_{\odot}$ and $1.0M_{\odot}$. We provide to `evolve_mf` the initial mass function slopes and breakpoints, the cluster age, metallicity and escape velocity, as well as parameters which control the mass loss due to escaping stars the specific binning to be used when the present day mass function is sampled. Figure 2.1 shows the evolution of a mass function over a span of 10 Gyr.

2.2.2 Binary Mass Functions

In order to include binary stars in our mass functions we make use of the assumption that for the vast majority of their interactions with other objects, binary systems behave essentially as point masses given the fact that they are tightly bound. This means that in order to replicate the effects of a binary population in our mass function, we simply need to shift some of the mass in single stars into heavier bins which act as the "binary bins".

We split this process up into several steps. First we divide the total binary fraction among the values if q in the requested mass ration distribution. We weight the f_b values assigned to the individual values of q by the chosen mass ration distribution, so a flat mass ratio distribution would have the total binary fraction divided evenly among the values while a "solar distribution" (see Fisher et al. 2005) would have a

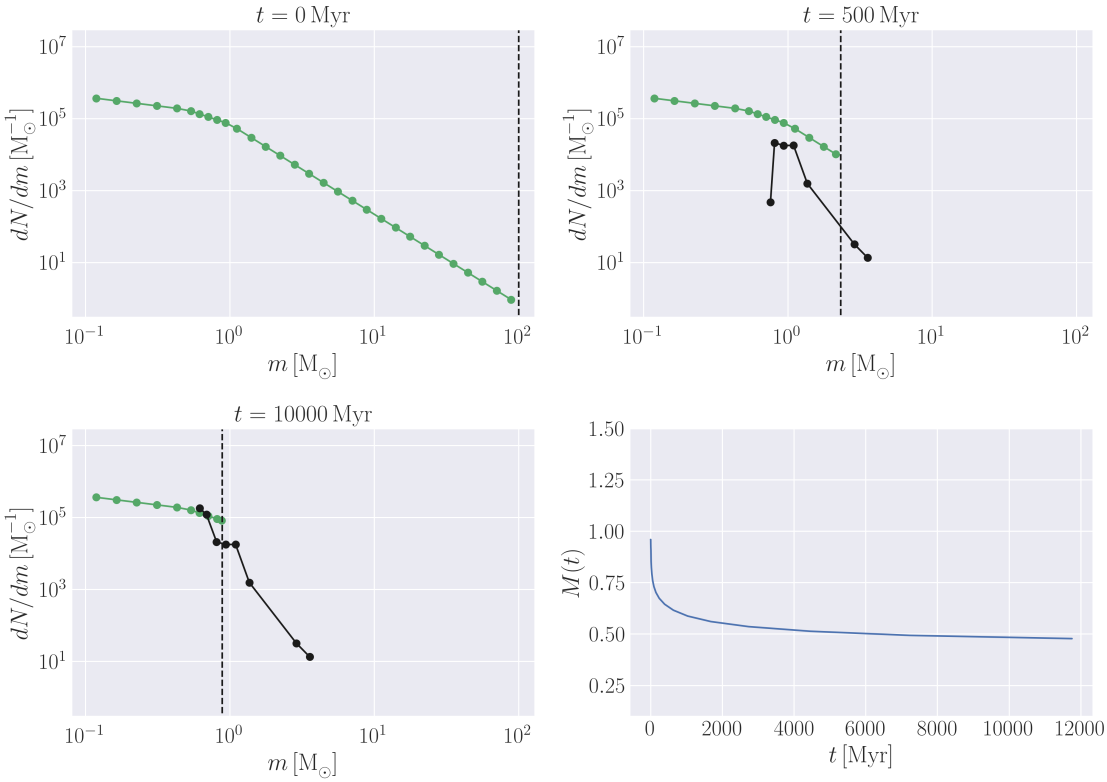

Figure 2.1: The evolution of a typical mass function from $t = 0$ to $t = 10000$ Myr. The stellar bins are plotted in green while the remnant bins are plotted in black, the current main-sequence turn-off is plotted a dashed black line. As the mass function ages, more and more main sequence stars evolve into remnants. Lower right: The evolution of the total mass of the mass function is plotted as a fraction of the initial mass. Mass loss is dominated by the effects of stellar evolution but also has contribution from dynamical ejected and escaping stars.

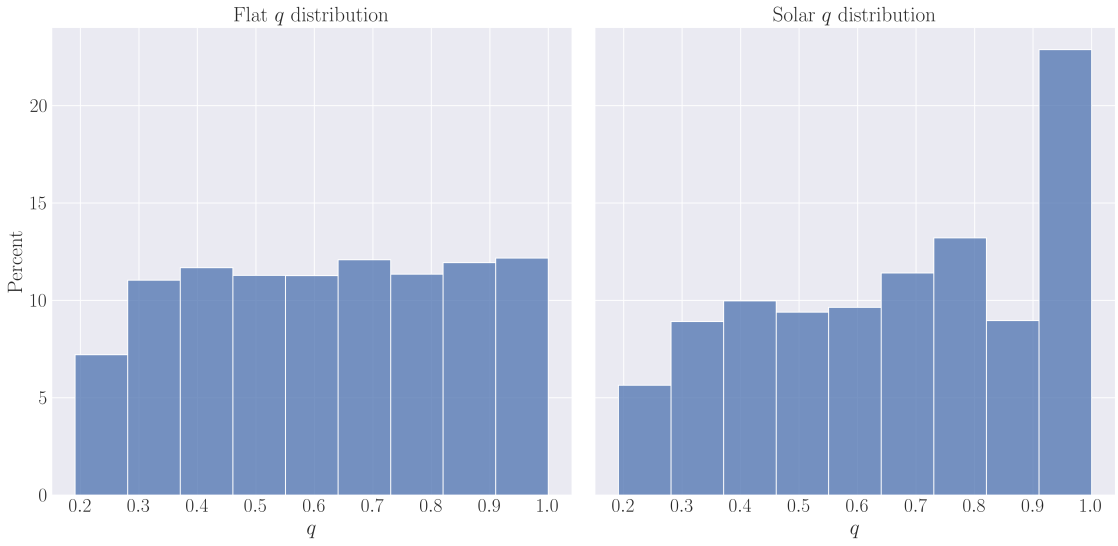

Figure 2.2: The resulting mass ratio distributions for the "flat" and "solar" mass ratio prescriptions. Both distributions are truncated and lowered at $q = 0.2$ due to the relative lack low very low mass stars within the mass functions, making the creation of very low q binaries impossible.

significantly higher portion of the total f_b assigned to equal mass binaries. Figure 2.2 shows the resulting mass ratio distributions using this method.

After we have calculated the individual binary fractions for each value of q, we then go through each bin of main sequence stars and attempt to make binaries. The companion mass for a given bin is calculated using the current value of q and the number of binaries to make is calculated using the binary fraction for the current value of q. After the companion mass and number of binaries are set, we then find the closest bin to the companion mass and subtract from the primary and companion bins the mass corresponding to the calculated number of binaries, adding the subtracted mass to a new bin with a mean mass equal to the sum of each binary component.

We repeat this process for each bin of main sequence stars until all bins have a binary fraction equal to that of the current value of q. We do this process for

each value of q in the mass ratio distribution, resulting in each main sequence bin having a binary fraction equal to the requested total binary fraction and a mass ratio distribution identical to the requested distribution.

This process tends to create on the order of 150 new bins in our mass function which dramatically increases the runtime of the `LIMEPY` models. In order to prevent this we group together binary bins of similar masses, forming on the order of 15 binary bins containing binary systems of similar total mass but differing mass ratios. Figure 2.3 shows the original main sequence bins, plotted with the modified main sequence bins, binary bins and rebinned binary bins.

2.3 Fitting Models to Data

To fit our models to the data we use the `GCfit` package[3]. `GCfit` provides a uniform interface for fitting `evolve_mf` and `LIMEPY` models to observations of clusters using either MCMC or Nested Sampling.

Peter: Here we should say if we use Nested Sampling or MCMC and why and what the setup is like.

2.3.1 Likelihoods

The majority of the likelihood functions we use are simple Gaussian likelihoods of the following form:

[3] `www.github.com/nmdickson/gcfit`

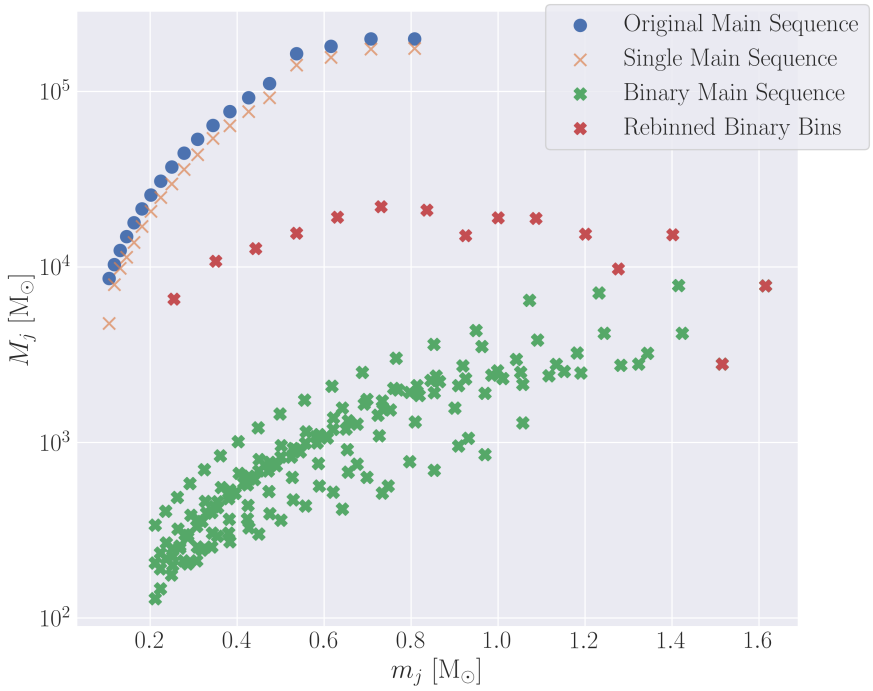

Figure 2.3: The main-sequence portion of a mass function before and after binaries are added. The blue circles are the original main sequence and the crosses are the modified main sequence. The orange crosses show the single stars after mass has been removed to create binaries and the many green crosses are the binary bins that are initially created. The red crosses are the rebinned binary bins which are actually used in the computation of the `LIMEPY` models.

$$\ln(\mathcal{L}) = \frac{1}{2}\sum_{r}\left(\frac{\left(\sigma_{\rm obs}(r) - \sigma_{\rm model}(r)\right)^2}{\delta\sigma^2_{\rm obs}(r)} - \ln\left(\delta\sigma^2_{\rm obs}(r)\right)\right) \tag{2.1}$$

Where $\mathcal{L}$ is the likelihood, σ is the line-of-sight velocity dispersion, r is the projected distance from the cluster centre, and $\delta\sigma$ is the uncertainty in the velocity dispersion. The likelihoods for other observables are formulated in the same way, and the specifics are discussed in `GCfit`'s documentation[4]. The total likelihood is therefore the sum of all the log-likelihoods for each set of observations.

For the mass function and number density likelihoods we include additional nuisance and scaling terms to account for extra sources of error in the mass function data and the effects of potential escapers at the cluster boundary.

2.3.2 Fitting Mass Functions to Observations

When the mass function data was originally collected, the mass was recorded based on the position of the star on an isochrone fit to the cluster. This means that any binary stars in the sample are recorded as single stars a mass corresponding to a star with the average colour of the two binary components and a luminosity corresponding to the sum of the two components.

Additionally, when we move mass around to create binary bins we remove mass from the surface density profiles which would be compared to the mass function data. In order to compensate for these effects, we rescale the surface density profiles to include the stars which are in binary bins, according to how they would have been

[4] `gcfit.readthedocs.io`

observed using the observational method described above.

In order to determine the observed mass we use a grid of MIST isochrones computed at a range of metallicities, at the age of the cluster. We use the isochrone to determine the luminosity of the binary components and then use the isochrone to determine the observed mass of the combined luminosities. We then scale the surface density profile of the main sequence bin which most closely matches the observed mass of the binary system by the total mass of the binary system which allows us to correct for both effects.

Chapter 3

Results

Chapter 4

Discussion

Appendix A

Appendix

Bibliography

F. Abbate, A. Possenti, A. Ridolfi, P. C.C. Freire, F. Camilo, R. N. Manchester, and N. D'Amico. Internal gas models and central black hole in 47 Tucanae using millisecond pulsars. *Monthly Notices of the Royal Astronomical Society*, 481(1):627–638, nov 2018.

H. Baumgardt. N-body modelling of globular clusters: Masses, mass-to-light ratios and intermediate-mass black holes. *Monthly Notices of the Royal Astronomical Society*, 464(2):2174–2202, jan 2017.

H. Baumgardt and M. Hilker. A catalogue of masses, structural parameters, and velocity dispersion profiles of 112 Milky Way globular clusters. *Monthly Notices of the Royal Astronomical Society*, 478(2):1520–1557, aug 2018.

A. Bellini, J. Anderson, R. P. Van Der Marel, L. L. Watkins, I. R. King, P. Bianchini, J. Chanamé, R. Chandar, A. M. Cool, F. R. Ferraro, H. Ford, and D. Massari. Hubble Space Telescope proper motion (HSTPROMO) catalogs of galactic globular clusters. I. Sample selection, data reduction, and NGC 7078 results. *Astrophysical Journal*, 797(2):115, dec 2014.

Sourav Chatterjee, Stefan Umbreit, John M. Fregeau, and Frederic A. Rasio. Understanding the dynamical state of globular clusters: Core-collapsed versus non-core-collapsed. *Monthly Notices of the Royal Astronomical Society*, 429(4):2881–2893, mar 2013.

T. J.L. De Boer, M. Gieles, E. Balbinot, V. Hénault-Brunet, A. Sollima, L. L. Watkins, and I. Claydon. Globular cluster number density profiles using Gaia DR2. *Monthly Notices of the Royal Astronomical Society*, 485(4):4906–4935, jun 2019.

James Fisher, Klaus Peter Schröder, and Robert Connon Smith. What a local sample of spectroscopic binaries can tell us about the field binary population. *Monthly Notices of the Royal Astronomical Society*, 361(2):495–503, aug 2005.

P. C.C. Freire, A. Ridolfi, M. Kramer, C. Jordan, R. N. Manchester, P. Torne, J. Sarkissian, C. O. Heinke, N. D'Amico, F. Camilo, D. R. Lorimer, and A. G. Lyne. Long-term observations of the pulsars in 47 Tucanae - II. Proper motions, accelerations and jerks. *Monthly Notices of the Royal Astronomical Society*, 471(1): 857–876, oct 2017.

Paulo C.C. Freire and Alessandro Ridolfi. An algorithm for determining the rotation count of pulsars. *Monthly Notices of the Royal Astronomical Society*, 476(4):4794–4805, feb 2018.

Mark Gieles, Eduardo Balbinot, Rashid I.S.M. Yaaqib, Vincent Hénault-Brunet, Alice Zocchi, Miklos Peuten, and Peter G. Jonker. Mass models of NGC6624 without an intermediate-mass black hole. *Monthly Notices of the Royal Astronomical Society*, 473(4):4832–4839, feb 2018.

Mark Gieles and Alice Zocchi. A family of lowered isothermal models. *Monthly Notices of the Royal Astronomical Society*, 454(1):576–592, nov 2015.

Mirek Giersz, Nathan Leigh, Arkadiusz Hypki, Nora Lützgendorf, and Abbas Askar. MOCCA code for star cluster simulations IV. A new scenario for intermediate mass black hole formation in globular clusters. *Monthly Notices of the Royal Astronomical Society*, 454(3):3150–3165, dec 2015.

Benjamin Giesers, Sebastian Kamann, Stefan Dreizler, Tim Oliver Husser, Abbas Askar, Fabian Göttgens, Jarle Brinchmann, Marilyn Latour, Peter M. Weilbacher, Martin Wendt, and Martin M. Roth. A stellar census in globular clusters with MUSE: Binaries in NGC 3201. *Astronomy and Astrophysics*, 632, dec 2019.

Douglas Heggie and Piet Hut. *The Gravitational MillionBody Problem*. Cambridge University Press, jan 2003.

Douglas C Heggie. Binary Evolution in Stellar Dynamics. *Monthly Notices of the Royal Astronomical Society*, 173(3):729–787, dec 1975.

V. Hénault-Brunet, M. Gieles, A. Sollima, L. L. Watkins, A. Zocchi, I. Claydon, E. Pancino, and H. Baumgardt. Mass modelling globular clusters in the Gaia era: A method comparison using mock data from an N-body simulation of M 4. *Monthly Notices of the Royal Astronomical Society*, 483(1):1400–1425, feb 2019.

V. Hénault-Brunet, M. Gieles, J. Strader, M. Peuten, E. Balbinot, and K. E.K. Douglas. On the black hole content and initial mass function of 47 Tuc. *Monthly Notices of the Royal Astronomical Society*, 491(1):113–128, jan 2020.

M. Hénon. Monte Carlo models of star clusters. *Astrophysics and Space Science*, 13 (2):284–299, oct 1971.

J. Heyl, I. Caiazzo, H. Richer, J. Anderson, J. Kalirai, and J. Parada. Deep HST Imaging in 47 Tucanae: A Global Dynamical Model . *The Astrophysical Journal*, 850(2):186, dec 2017.

Arkadiusz Hypki and Mirek Giersz. mocca code for star cluster simulations I. Blue stragglers, first results. *Monthly Notices of the Royal Astronomical Society*, 429(2): 1221–1243, feb 2013.

Ivan R. King. The structure of star clusters. III. Some simple dvriamical models. *The Astronomical Journal*, 71(1):64, 1966.

Kyle Kremer, Claire S. Ye, Sourav Chatterjee, Carl L. Rodriguez, and Frederic A. Rasio. The Role of black hole burning in the evolution of dense star clusters. *Proceedings of the International Astronomical Union*, 14(S351):357–366, may 2019.

A. P. Milone, G. Piotto, L. R. Bedin, A. Aparicio, J. Anderson, A. Sarajedini, A. F. Marino, A. Moretti, M. B. Davies, B. Chaboyer, A. Dotter, M. Hempel, A. Marín-Franch, S. Majewski, N. E.Q. Paust, I. N. Reid, A. Rosenberg, and M. Siegel. The ACS survey of Galactic globular clusters: XII. Photometric binaries along the main sequence. *Astronomy and Astrophysics*, 540(S241):A16, apr 2012.

M. Peuten, A. Zocchi, M. Gieles, and V. Hénault-Brunet. Testing lowered isothermal models with direct N-body simulations of globular clusters - II. Multimass models. *Monthly Notices of the Royal Astronomical Society*, 470(3):2736–2761, sep 2017.

A. Ridolfi, P. C.C. Freire, P. Torne, C. O. Heinke, M. van den Berg, C. Jordan, M. Kramer, C. G. Bassa, J. Sarkissian, N. D'Amico, D. Lorimer, F. Camilo, R. N. Manchester, and A. Lyne. Long-term observations of the pulsars in 47 Tucanae - I. A study of four elusive binary systems. *Monthly Notices of the Royal Astronomical Society*, 462(3):2918–2933, nov 2016.

Carl L. Rodriguez, Newlin C. Weatherford, Scott C. Coughlin, Pau Amaro Seoane, Katelyn Breivik, Sourav Chatterjee, Giacomo Fragione, Fulya Krolu, Kyle Kremer, Nicholas Z. Rui, Claire S. Ye, Michael Zevin, and Frederic A. Rasio. Modeling Dense Star Clusters in the Milky Way and Beyond with the Cluster Monte Carlo Code. jun 2021.

A. Sollima and H. Baumgardt. The global mass functions of 35 Galactic globular clusters: I. Observational data and correlations with cluster parameters. *Monthly Notices of the Royal Astronomical Society*, 471(3):3668–3679, nov 2017.

Laura L. Watkins, Roeland P. Van Der Marel, Andrea Bellini, and Jay Anderson. HUBBLE SPACE TELESCOPE PROPER MOTION (HSTPROMO) CATALOGS of GALACTIC GLOBULAR CLUSTERS. III. DYNAMICAL DISTANCES and MASS-TO-LIGHT RATIOs. *Astrophysical Journal*, 812(2):149, oct 2015.

C. P. Wilson. Dynamical models of elliptical galaxies. *The Astronomical Journal*, 80:175, mar 1975.

R. v. d. R. Woolley. A Study of the Equilibrium of Globular Clusters. *Monthly Notices of the Royal Astronomical Society*, 114(2):191–209, apr 1954.

Alice Zocchi, Mark Gieles, and Vincent Hénault-Brunet. Radial anisotropy in ω Cen limiting the room for an intermediate-mass black hole. *Monthly Notices of the Royal Astronomical Society*, 468(4):4429–4440, jul 2017.

Alice Zocchi, Mark Gieles, Vincent Hénault-Brunet, and Anna Lisa Varri. Testing lowered isothermal models with direct N-body simulations of globular clusters. *Monthly Notices of the Royal Astronomical Society*, 462(1):696–714, oct 2016.